



Published in final edited form as:

J Med Chem. 2008 April 10; 51(7): 2088–2099. doi:10.1021/jm701442d.

Probing Distal Regions of the A_{2B} Adenosine Receptor by Quantitative Structure-Activity Relationship Modeling of Known and Novel Agonists

Andrei A. Ivanov, Ben Wang, Athena M. Klutz, Vincent L. Chen, Zhan-Guo Gao, and Kenneth A. Jacobson*

Molecular Recognition Section, Laboratory of Bioorganic Chemistry, National Institute of Diabetes and Digestive and Kidney Diseases, National Institutes of Health, Bethesda, Maryland 20892

Abstract

The binding modes at the A_{2B} adenosine receptor (AR) of 72 derivatives of adenosine and its 5'-*N*-methyluronamide with diverse substitutions at the 2 and N⁶ positions were studied using a molecular modeling approach. The compounds in their receptor-docked conformations were used to build CoMFA and CoMSIA quantitative structure–activity relationship models. Various parameters, including different types of atomic charges, were examined. The best statistical parameters were obtained with a joint CoMFA and CoMSIA model: R^2) 0.960, Q^2) 0.676, SEE) 0.175, F) 158, and R^2_{test}) 0.782 for an independent test set containing 18 compounds. On the basis of the modeling results, four novel adenosine analogues, having elongated or bulky substitutions at N⁶ position and/or 2 position, were synthesized and evaluated biologically. All of the proposed compounds were potent, full agonists at the A_{2B} AR in adenylate cyclase studies. Thus, in support of the modeling, bulky substitutions at both positions did not prevent A_{2B} AR activation, which predicts separate regions for docking of these moieties.

Introduction

The A_{2B} adenosine receptor (AR)^a is one of the four known subtypes of ARs: A₁, A_{2A}, A_{2B}, and A₃. These receptors are members of the rhodopsin family of G-protein-coupled receptors (GPCRs).^{1–3} A_{2B} AR agonists are of interest in the treatment of diseases such as cardiac ischemia and diabetes.^{4,5}

*To whom correspondence should be addressed. Phone: (301) 496-9024. Fax: (301) 480-8422. kajacobs@helix.nih.gov.

Supporting Information Available: Table of A_{2B} AR ligands in the training and test sets, adenylate cyclase concentration–response curves, and HPLC analysis results of the newly synthesized nucleosides **7–10**. This material is available free of charge via the Internet at <http://pubs.acs.org>.

^aAR, adenosine receptor; CoMFA, comparative molecular field analysis; CoMSIA, comparative molecular similarity indices analysis; CPA, N⁶-cyclopentyladenosine; EL, extracellular loop; GPCR, G-protein-coupled receptor; HENECA, 2-(1-(*E*)-hexenyl)adenosine-5'-*N*-ethyluronamide; MCMM, Monte Carlo multiple minimum; NECA, 5'-*N*-ethylcarboxamidoadenosine; (*S*)-PHPAdo, (*S*)-2-[(3-hydroxy-3-phenyl)propyn-1-yl]adenosine; (*S*)-PHPNECA, (*S*)-2-[(3-hydroxy-3-phenyl)propyn-1-yl]-5'-*N*-ethylcarboxamidoadenosine; PLS, partial least squares; HBD, hydrogen bond donor; HBA, hydrogen bond acceptor; RP, relative potency; DS, data set; QSAR, quantitative structure–activity relationship; TM, transmembrane helical domain; PyBop, benzotriazol-1-yloxytripyrrolidinophosphonium hexafluorophosphate; DIPEA, diisopropylethylamine; DMF, *N,N*-dimethylformamide; HRMS, high-resolution mass spectrometry; TEA, triethylamine; TLC, thin layer chromatography.

Like other members of the class A GPCR family, ARs are transmembrane proteins containing the typical seven transmembrane R-helical domains (TM I–VII) as well as extracellular (EL) and intracellular (IL) loops. X-ray crystallographic data are available for only a few GPCRs, i.e., rhodopsin and the β_2 -adrenergic receptor; the experimental three-dimensional structures of the ARs are unknown. Therefore, the homology modeling approach is commonly used to study the structure and ligand–receptor interactions of various GPCRs and other proteins.^{6–9} Several rhodopsin-based molecular models of the A₁, A_{2A}, A_{2B} and A₃ ARs have been proposed. The SAR (structure–activity relationship) of adenosine derivatives acting as A_{2B} AR agonists has been studied qualitatively (representative reference structures in Chart 1). Recently we have published a model of the A_{2B} AR complex with its potent agonist MRS3997 **4**.¹⁶

Since molecular models can provide information about ligand–receptor interactions, quantitative SAR (QSAR) statistical models are widely used to evaluate the activity or other properties of known ligands and in virtual screening.^{17,18} QSAR models are useful to explore the contribution of specific functional groups and moieties on the ligand to the overall biological activity. The comparative molecular field analysis (CoMFA) and comparative molecular similarity indices analysis (CoMSIA) are two of the most effective and descriptive methods of QSAR-modeling.¹⁹ CoMFA/CoMSIA in conjunction with receptor docking has been used to study the binding of agonists²⁰ and antagonists^{21,22} at the human A₃ AR. CoMFA has also been used to study ligand recognition at other ARs.^{23,24}

Recently, novel adenosine derivatives substituted at the N⁶ and/or 5' positions or at the C2 position were reported to be potent and/or selective A_{2B} AR agonists (Chart 1).^{16,25,26} In the present study we have synthesized new analogues in which several of these affinity-(or selectivity-) enhancing substituents have been recombined in order to probe the compatibility of multiple extended groups in receptor docking and activation. Previous studies have reported that certain combinations of otherwise affinity-enhancing substitutions at the N⁶ and C2 positions were incompatible in binding to a given AR subtype.^{16,27,28} Here, the molecular docking at the A_{2B} AR of both previously reported and novel derivatives of adenosine and the potent, nonselective agonist 5'-N-ethylcarboxamidoadenosine (NECA, **1**) combined with the CoMFA and CoMSIA modeling was used to characterize the distal regions of the receptor involved in ligand recognition.

Results and Discussion

A_{2B} Agonists Binding Mode.

For a long time within the superfamily of GPCRs, an X-ray structure was available for rhodopsin only.^{29,30} Very recently Kobilka and co-workers reported the first X-ray structure of the β_2 -adrenergic receptor.⁵³ However, the structure of other GPCRs and their ligand–receptor complexes can be studied with the rhodopsin-based homology modeling approach.^{31,32} In this paper, our previously published molecular model of the human A_{2B} AR^{15,16} was used to study the binding modes of various well-known and recently proposed agonists of the A_{2B} AR. The A_{2B} AR model was built in homology with the X-ray structure of bovine rhodopsin and contains all seven transmembrane R-helices, as well as the intracellular and the extracellular hydrophilic loops.

Adenine and Ribose Moieties in the Putative Receptor Binding Site.

Prior to the building of the CoMFA and CoMSIA quantitative structure–activity relationship models, the receptor-docked conformations of the nucleoside ligands were calculated. Unfortunately, the X-ray structure of rhodopsin that serves as the template for our GPCR models was obtained for its ground state only. For this reason, there is an opinion that rhodopsin-based homology modeling of GPCRs is more applicable for studying antagonist than agonist binding modes. On the other hand successful docking studies of agonists were reported for various rhodopsin-based models of GPCRs. It was demonstrated that differences in the binding site configuration in the active and inactive states of the receptor can be taken into account using protein-flexible docking or conformational search analysis.^{6,12,14} In this study the putative binding modes of various agonists (**1-6**, **11-76**) of the A_{2B} AR (2- and N⁶-substituted analogues of adenosine and **1**) were studied with the Monte Carlo multiple minimum (MCMM) conformational search analysis applied to the ligand docked to the binding site of the receptor. The structures of all ligands used in the study with their experimental and predicted activities are given in the Supporting Information. MacroModel software was used for automated docking.³³

The results obtained indicated that the adenosine moiety of all studied ligands had a similar position and orientation inside the putative binding site. In particular, the N⁶-amino group of the ligands was oriented toward TM V, and position 2 of the adenine ring was oriented toward EL2. The 5' position of the ribose ring and the N⁶ substituent, when present, were oriented toward the intracellular part of the receptor (Figure 1).

A schematic representation of the ligand binding mode at the putative nucleoside binding site of the human A_{2B} AR is shown in Figure 2. In agreement with the published data of molecular modeling and site-directed mutagenesis of the AR family,^{12,14–16,34} the 2'- and 3'-hydroxyl groups of the docked nucleosides could form H-bonds with the conserved His280^{7,43}. In addition, Thr89^{3,36} was involved in H-bonding with the oxygen atom of the ribose ring and the 5'-hydroxyl group of adenosine analogues. The 5'-NH-group of 5'-N-alkylcarboxamido adenosine derivatives also formed an H-bond with Thr89^{3,36}, while the oxygen atom of the 5'-amido group was H-bonded to Ser279^{7,42}. The side chains of Asn186^{5,42} and Asn254^{6,55} were observed in proximity to the adenine ring of the ligands. Also, Trp247^{6,48} and His251^{6,52} were located near the N⁶ and 7 positions of the adenine ring, in agreement with previous studies.¹² On the basis of the data of site-directed mutagenesis of other ARs, all of these conserved residues were reported to be critical for ligand binding.³⁴

Detailed Interactions of N⁶- and 2-Substituted Derivatives of Adenosine and **1**.

The binding modes of various N⁶-substituted analogues of adenosine and **1** at the A_{2B} AR were studied using MCMM calculations. As already mentioned, the N⁶ position of the ligands was oriented toward TM V. In addition, the N⁶-amino group appeared in proximity to the side chain of Asn254^{6,55}, with which it likely could form an H-bond. This observation confirmed the previously published results of molecular modeling of ARs.^{15,16} However, extended groups at the N⁶ position, in particular N⁶-arylcarbonylmethoxyphenyl or N⁶-(arylcarbonyl)hydrazino groups, present in recently reported A_{2B} AR agonists,^{25,26} were

found to be oriented toward the intracellular region of the receptor. Interestingly, previous modeling studies indicated that similar groups at the 8 position of some xanthine antagonists of the A_{2B} AR could be oriented in the opposite direction, i.e., toward the extracellular region.^{10,11} In this study the MCMC calculations performed for such agonists were initiated from various starting points with various randomly generated initial orientations of the N⁶ substituent. The results obtained indicated that the orientation of this group toward the intracellular region was the most favorable energetically. Moreover, in those cases when the opposite orientation of the long N⁶ substituent was observed, critical ligand–receptor interactions were lost. In particular, in such cases the 2'- and 3'-hydroxyl groups were not involved in H-bonding with His280^{7,43}, and the H-bonds with Thr89^{3,36} were lost.

In the models obtained for N⁶-arylcarbonylmethoxyphenyl derivatives such as **6**, neither the amido group of this chain nor its ether oxygen atom was involved in H-bonding. However, the backbone oxygen atoms of Cys190^{5,46} and Val191^{5,47} were located in proximity to these groups. The terminal aromatic ring of the N⁶ substituent was favorably located in the pocket formed by several hydrophobic residues including Pro194^{5,50}, Leu195^{5,51}, Met198^{5,54}, Phe243^{6,44}, and Ala244^{6,45}.

On the basis of the models obtained, the arylcarbonyl oxygen atom of N⁶-(arylcarbonyl)hydrazino derivatives, such as **5**, can form a H-bond with His251^{6,52}. In addition, it was found that the oxygen atom of the furan ring of such compounds could form a weak H-bond with the NH-group of the indole ring of Trp247^{6,48}.

In summary, in our docking hypothesis the substituent at the 2 position was oriented toward the extracellular loops and the N⁶ substituent toward TM V, in the direction of the cytosolic side of the receptor. The binding modes obtained for known 2-substituted derivatives of adenosine and **1** such as **2**, **4**, **16**, **18–26**, **28**, **33–47** were the same as we reported previously.^{15,16}

QSAR Models.

Statistical models of quantitative structure–activity or structure–property relationships (QSAR/QSPR) are widely used to evaluate computationally various properties of chemical structures.^{35–37} In particular, such methods are useful to evaluate and predict the ligand potency or activity. Numerous approaches to build QSAR models have been introduced.^{38–42} Most of these approaches are based on multiple linear-regression analysis or on partial least-squares (PLS) analysis. They use a number of independent variables, i.e., descriptors calculated from the molecular structure, to obtain a reasonable correlation with a dependent variable, the studied biological property.

In the present study, CoMFA and CoMSIA implemented in Sybyl 7.3⁴³ were utilized to build statistically reliable “structure–potency” models for agonists of the human A_{2B} AR. Both CoMFA and CoMSIA approaches are based on the PLS analysis.^{44,45} To build the CoMFA or CoMSIA model, an alignment of the studied compounds is needed. Since the initial model of the A_{2B} AR used for the ligand docking had the same coordinates for all compounds, a reasonable and receptor-related alignment was obtained automatically after the docking studies (Figure 2). The relative potency (RP) with respect to **1** was calculated

for each compound as described in the Experimental Section, and it was used as the dependent variable in QSAR models. Then the steric and electrostatic CoMFA contours as well as electrostatic, H-bond donor (HBD) and acceptor (HBA), and hydrophobic CoMSIA contours were calculated with Sybyl7.3.

Individual CoMFA and CoMSIA and joint CoMFA/CoMSIA models were built for the training set of 54 randomly selected A_{2B} AR agonists, for which data in the stimulation of adenylate cyclase has been reported (Table 1 and Tables S1 and S2 of Supporting Information). The four different types of partial atomic charges, namely, Gasteiger-Hückel, AM1, PM3, and MNDO, were used. Initially the lattice spacing of 2 Å and only electrostatic, HBA, and HBD but not hydrophobic CoMSIA contours were calculated. The results obtained for a succession of models are summarized in Table 1. The best CoMFA model was derived for the data set (DS) of compounds with AM1 partial charges (Q^2)=0.585, R^2)=0.914, standard error of estimation (SEE)=0.252, F =102; PLS components (C)=5). In contrast, the best statistical parameters of the CoMSIA models were obtained for the compounds with the PM3 atomic charges (Q^2)=0.612, R^2)=0.917, SEE)=0.253, F)=73, C)=7). Both AM1 and PM3 partial atomic charges provided reasonable statistical parameters of the joint CoMFA/CoMSIA models. However, the best results were obtained for the set of compounds with the MNDO charges assigned (Q^2)=0.649, R^2)=0.958, SEE)=0.182, F)=128, C)=8). Also, as follows from the data, the joint CoMFA/CoMSIA model allowed a better correlation and error of estimation in comparison with individual CoMFA and CoMSIA models. It is known that in some cases the quality of a CoMFA/CoMSIA model can be significantly improved using a decreased value of the lattice spacing. To examine this possibility, the joint CoMFA/CoMSIA model derived for the MNDO-charged compounds was rebuilt with a lattice spacing of 1 Å. This model (model 1) was characterized by the following improved statistical parameters: Q^2)=0.668, R^2)=0.963, SEE)=0.171, F)=146, C)=8. The value of the regression coefficient obtained for the independent test set of 18 compounds (indicated in Table S2 of Supporting Information) was as high as R^2_{test})=0.714.

Then with the aim of improving the model quality, the hydrophobic CoMSIA contours were taken into account to provide model 2. The lattice spacing of 1 Å and MNDO partial atomic charges were used. The optimal number of PLS components was found to be C)=7. The addition of the hydrophobic CoMSIA regions resulted in slightly decreased values of the regression coefficient (R^2)=0.952) and Fisher's criterion (F)=131). Also, the value of standard error of estimation was increased (SEE)=0.192). However, the value of leave-one-out cross-validated correlation coefficient (Q^2)=0.691) was found to be higher than in model 1, demonstrating the better stability of model 2. Moreover, the regression coefficient obtained for the independent test set of compounds was also higher in model 2 (R^2_{test})=0.759) than in model 1 (R^2)=0.714). As a final step of the model refinement, model 2 was rebuilt with the attenuation factor (R) increased from its standard value of 0.30 to 0.50. The higher value of the attenuation factor provided more detailed and localized CoMSIA contours.⁴⁵ Model 3 was obtained and characterized by the following statistical parameters: R^2)=0.960, Q^2)=0.676, SEE)=0.176, F)=158, C)=7, R^2_{test})=0.782. The higher value of the attenuation factor provided a further improvement of the model statistics, namely, a higher value of the regression coefficient for the test set, a lower value of SEE, and

optimal values of R^2 and Q^2 coefficients. Also the F criterion was increased. As shown in Figure 3, all points on the correlation plot fit well with the ideal line for both training and test sets of compounds, and no outliers were observed. Since the statistical parameters of model 3 were found to be reasonable, a further refinement of the model quality was not performed.

CoMFA Regions. CoMFA Steric Regions.

In agreement with experimentally determined ligand potencies at the A_{2B} AR, bulky groups were predicted to be favorable around the indolyl ring of 2-(3-(indolyl)ethoxy) derivatives such as MRS3997 **4** (Figure 4A, region i). In contrast, the existence of bulky groups between the indole ring and the 2 position of the adenine ring was predicted to be less favorable (Figure 4A, region ii). Those conditions are reflected in the experimental data, particularly with the low potency of 2-chloro substituted derivatives and compounds with an alkyl chain at the 2 position. The unfavorable region for bulky groups (yellow region iii) was also observed near the N⁶ position of the ligands. This region corresponds to weak N⁶ substituted ligands, for example, N⁶-cyclopentyl, N⁶-isopropyl, or N⁶-ethyl derivatives. However, because of the presence of more potent N⁶-(arylcarbonyl)hydrazino substituted derivatives of **1**, the favorable bulky group area iv appeared just below the unfavorable yellow region iii (Figure 4A). The green area v in the lower part of Figure 4A corresponds to the terminal aryl ring of N⁶-arylcarbamoylmethoxyphenyl derivatives, namely, **6**, **58**, **60–62**, **64–66**.

In contrast to N⁶-arylcarbamoylmethoxyphenyl-substituted derivatives, benzyl- or cyclohexyl-substituted compounds (such as **70**, **72**, **76**) are generally less potent at the A_{2B} AR. For this reason, the areavi occupied by those groups was recognized by the model as unfavorable (yellow) for the bulky groups.

CoMFA Electrostatic Regions.

The 2-chloro substituted derivatives of adenosine and **1** (e.g., pEC₅₀ (**51**)= -2.322, pEC₅₀ (**73**)= -1.629) are less potent at the A_{2B} AR than the corresponding compounds unsubstituted at the 2 position (e.g., pEC₅₀ (**5**)= -1.914, pEC₅₀ (**73**)= -0.863). Since a chlorine atom has a negative partial atomic charge, more positively charged groups were predicted to be favorable near position 2 of the adenine ring (Figure 4B, region i).

In contrast, the red region ii, which is favorable for the less negatively charged groups, was derived in the upper part of Figure 4B. This red area corresponds to the hydroxyl group of the 2-(3-hydroxy-3-phenyl) propyn-1-yl moiety of (*S*)-PHPNECA **2** and (*S*)-PHPAdo **33**. Also, the region iii of the favorable position of more negatively charged atoms appeared just below the N⁶-amino group of the studied compounds. This area corresponds to the carbonyl oxygen atom and the oxygen atom of the furanyl ring of the N⁶-(arylcarbonyl)hydrazino derivatives such as **5**.

In addition, positively charged groups were predicted to be favorable in proximity to the distal NH group of the N⁶-arylcarbamoylmethoxyphenyl derivatives such as **6** (Figure 4B, region iv). Additional negatively charged groups were predicted to be favorable in proximity to the oxygen atom of the arylcarbamoil moiety in this series (region v).

CoMSIA Regions.

The CoMSIA steric and electrostatic contours were found to be nearly identical to the corresponding CoMFA contours. Since these contours were discussed above, the following section will concern the CoMSIA H-bond donor and acceptor contours as well as the CoMSIA hydrophobic contours.

CoMSIA H-Bond Donor and Acceptor Regions.

To take into account the role of H-bond donor and acceptor groups of the compounds, the corresponding CoMSIA contours were calculated. The CoMSIA acceptor contour corresponds to the H-bond donating groups of the receptor, and similarly, the CoMSIA donor contour describes the regions where the H-bond acceptor groups of the receptor should be located.

As shown in Figure 5A, H-bond donating groups of the receptor were predicted to be favorable in proximity to the oxygen atoms of the hydroxyl group of the 2-(3-hydroxy-3-phenyl)propyn-1-yl moiety of (*S*)-PHPNECA **2** and (*S*)-PHPAdo **33** (orange region i). A second region (ii) favorable for receptor H-bond donating groups appeared between the ribose oxygen atom and the 5'-OH group of the adenosine derivatives.

Since the morpholino-substituted analogue **68** is one of the weak compounds in the series of *N*⁶-arylcarbamoylmethoxyphenyl derivatives, the oxygen atom of the morpholine ring was recognized as a disfavored feature by the model. For this reason, the location of the receptor H-bond donating groups was predicted to be unfavorable near that oxygen atom (red region iii in the bottom part of Figure 5A). A second red region (iv) in the bottom part of the Figure 5A was derived from the presence of *N*⁶-arylcarbamoylmethoxyphenyl derivatives containing methoxy groups at positions 3, 4, and 5 of the phenyl ring. These compounds are weaker than unsubstituted compound **6** (Chart1) or 4-phenyl substituted derivatives. For this reason, the model considered methoxy groups at those positions of the phenyl ring as unfavorable modifications. The red contour appearing near the *N*⁶-phenyl ring (Figure 5A, region v) reflects the sulfo group of *N*⁶-(4-sulfophenyl)adenosine (SPA) **32**, which also binds weakly at the A_{2B} AR.

Several regions that were unfavorable for the occurrence of H-bond donating groups on the receptor appeared around the ribose and adenine rings of the ligands(vi). However, these regions do not correspond to any unique structural features of individual ligands. It was found that, in general, the adenosine moieties of small nucleosides that were weak ligands of the A_{2B} AR, namely, *N*⁶-cyclopentyladenosine (CPA) **3**, **32**, and some other derivatives, were located deeper inside the receptor than the corresponding moiety of more potent, larger ligands, for example, compound **1** or **6**. The positions of the functional groups of the ribose moiety varied in the models obtained for various compounds. These differences were taken into account and resulted in the corresponding regionvi (Figure 5A).

For similar reasons, multiple regions that were unfavorable for H-bond acceptors on the receptor were derived in proximity to the ribose ring of the ligands.

In addition, as shown in Figure 5A, the position of the N^6 -amino group was found to be different for various ligands. In particular, the N^6 position of the adenine ring of **3** had the same position as adenine N1 of compound **6**. For this reason, regions where H-bond acceptor groups on the receptor are predicted to decrease the potency appeared in proximity to the N^6 and 1 positions of the ligands (regions vii, viii).

Interestingly, it was observed after the docking studies that the phenylcarbamoyl moiety of the less potent N^6 -arylcarbamoylmethoxybenzyl derivatives, namely, **70** included in the training set, appeared slightly deeper inside the receptor than this moiety of more potent N^6 -arylcarbamoylmethoxyphenyl derivatives (e.g., **6**). This difference in the ligand binding modes was characterized by two polyhedra in the CoMSIA model that appeared near the NH group of those compounds. The purple area ix, unfavorable for H-bond acceptor groups on the receptor, was located deeper than the area x that was favorable for such groups (cyan). The regions xi and xii, favoring H-bond acceptors on the receptor, were predicted to be near the 2'- and 3'-hydroxyl groups and the N^6 -amino group of the potent ligands of the $A_{2B}AR$.

CoMSIA Hydrophobic Regions.

Not surprisingly, the calculated CoMSIA hydrophobic contours are in a good agreement with the experimentally observed potencies of the studied compounds and their binding modes proposed with the molecular modeling (Figure 5B). Region i, unfavorable for hydrophobic groups on the receptor, appeared in proximity to the 5' region, i.e., consisting of a hydroxyl group for derivatives of adenosine or an NH group for **1**. Also, the presence of hydrophobic groups in positions occupied by 2'- and 3'-hydroxyl groups was predicted to be unfavorable (region ii). In addition, hydrophobic groups at the N^6 position were predicted to be unfavorable (region iii). These findings are in agreement with experimental values of EC_{50} of N^6 -methyl-(e.g., **29**, **39**, **46**), N^6 -ethyl (e.g., **35**, **36**, **40**), N^6 -isopropyl (e.g., **44**, **47**) derivatives, CPA **3**, and N^6 -phenyladenosine **30**. The small white area iv located below the N^6 position in Figure 5B was placed between the aromatic ring of N^6 -benzyladenosine **31** and the aromatic ring of compound **5** and its derivatives.

As shown in Figure 5B, the hydrophilic oxygen atom at position 4 of the phenyl ring of compound **6** was recognized by the model, and the corresponding hydrophobic disfavored region v appeared at that position.

The favored hydrophobic region vi appeared near the aromatic ring of the arylcarbamoyl moiety of **6**, indicating a lower potency of compounds with more hydrophilic methoxy groups in comparison with the unsubstituted phenyl ring or 4-halogenophenyl substituted derivatives.

One favored region (vii) and one disfavored region (viii) appeared in the upper part of Figure 5B. The favored (yellow) region vii corresponds to the aromatic rings of 2-(3-(indolyl)ethoxy) substituted adenosine derivatives (e.g., **4**), and to the phenyl ring of PHPNECA and PHPAdo analogues such as **2** and **34**. In contrast, the disfavored (white) region viii was located at the position of the long alkyl chain of 2-hexynyl substituted adenosine derivatives (**38**, **40**, **41**) and 2-(1-(*E*-hexenyl)adenosine-5'-*N*-ethyluronamide (HENECA) **45**. Also, a disfavored hydrophobic region appeared in proximity to the hydroxyl group of the 2-(3-hydroxy-3-

phenyl)propyn-1-yl moiety of (*S*)-PHPNECA **2** and (*S*)-PHPAdo **34**. In addition, the area occupied by the oxygen atom of the ethoxy group of 2-(3-(indolyl) ethoxy) substituted analogues (e.g., **4**, **16**, **20**, **22**) was recognized as a disfavored region (x) for hydrophobic groups, while a favored region appeared near position 2 of PHPNECA and PHPAdo analogues (Figure 5B).

Novel A_{2B} AR Agonists.

The analysis of the ligand binding modes obtained after the MCMM calculations were performed for the known A_{2B} AR agonists indicated that the substituents at the N⁶- and 2 positions were located in two distinct pockets of the binding site. As already discussed, the groups at the N⁶ position were oriented toward the intracellular region. In contrast, the substituents at position 2 were oriented toward the extracellular loops of the receptor. At the same time, the adenosine moiety had almost the same position inside the receptor for all of the studied ligands. These observations made it possible to propose that the ligands containing both extended groups at the N⁶ position^{25,26} and a bulky substituent at position 2, namely, a 2-(3-(indolyl)ethoxy) group as occurs in **4**,¹⁶ could also fit the binding site well. The findings stand in contrast to previous models that suggest an overlay between bulky substituents at the 2 and N⁶ positions.²⁷ We have found that in the present A_{2B} AR model these groups occupy distinct regions inside the binding site.

With the aim to test the above hypothesis, four novel adenosine derivatives **7–10** were designed and synthesized as potential agonists of the A_{2B} AR (Table 2). The synthetic routes are shown in Schemes 1 and 2. These structures were first docked to the A_{2B} AR model with the protocol used for all other studied ligands. All four compounds fit the binding site well and established similar ligand–receptor interactions as the corresponding individually substituted compounds (Figure 2).

The RP of these four novel agonists was predicted using the CoMFA/CoMSIA model 3. The results obtained are summarized in Table 2. In general, all compounds were predicted to be potent. As expected, compound **9**, the combination of the two most potent ligands **6** and **4**, was predicted as the most potent agonist. For similar reasons, a high potency was predicted for **10**.

The experimental values of EC₅₀ demonstrated that in agreement with the docking studies all compounds bound to the A_{2B} receptor. Also, the experimentally measured potency of these ligands indicated that all of them are potent agonists of the A_{2B} AR. Ligand **10** was found to be weaker than the other three novel compounds (EC₅₀) 965 nM). However, the selectivity of compounds **7–10** for the A_{2B} AR was low in comparison to the human A₁ and A_{2A} ARs (Table 2).

Thus, in the present study, the computational design of four novel agonists of the A_{2B} receptor was performed on the basis of the molecular and statistical modeling of the A_{2B} AR and its known ligands. These compounds were successfully synthesized and biologically evaluated at the human A_{2B} AR. The results revealed that all of the proposed compounds are moderately potent but nonselective agonists of the A_{2B} AR.

Conclusions

We utilized a molecular modeling approach to study putative binding modes of various N^6 - and 2-substituted derivatives of adenosine and its 5'-*N*-methyluronamide **1** at the human A_{2B} AR. The modeling results suggest that bulky substituents at the 2 and N^6 positions occupy distinct and nonoverlapping subregions within the putative A_{2B} AR binding site. Furthermore, these groups were oriented in opposite directions inside the binding pocket. The similarity and differences in the binding modes of the studied compounds were analyzed on the basis of the ligand–receptor models obtained.

A successful statistical CoMFA/CoMSIA model was derived for the NECA-related potency of the studied A_{2B} receptor agonists based on their receptor-docked conformation. The distribution of steric, electrostatic, H-bond donor and acceptor, and hydrophobic contours around the ligands was analyzed. The best statistical parameters were obtained with a joint CoMFA and CoMSIA model, which displayed an R^2 of 0.960. On the basis of the modeling results, four novel adenosine analogues having elongated substitutions at the N^6 and/or 2 positions were synthesized and evaluated biologically. All of proposed compounds were shown to be moderately potent, full agonists of the A_{2B} AR in adenylate cyclase studies. Thus, as predicted by the QSAR modeling in conjunction with receptor docking, combinations of elongated and bulky substituents in adenosine analogues are tolerated for recognition by the A_{2B} AR. These substituents bind to distinct pockets in the putative binding site for nucleosides in the TM region of the receptor. The QSAR models were consistent with the orientation of the N^6 -amino group toward TM V and the substituent at the adenine 2 position toward EL2.

Experimental Section

Data Set of Compounds.

The structures and experimental values of EC_{50} of 72 known agonists of the adenosine A_{2B} AR were collected from the literature.^{16,25,26,46–48} The 2- and N^6 -substituted derivatives of adenosine and NECA **1** were included in the DS. Since the EC_{50} values were measured with different protocols in various publications, the RP of compounds was calculated as $RP = pEC_{50}(\text{comp})_i - pEC_{50}(\text{NECA})_i$, where i represents the same reference publication. The entire DS was randomly divided into the test set of 54 compounds and training set of 18 compounds (25% of the total number of compounds). All types of compounds included in the entire DS were also included in both training and test sets of compounds.

The entire DS of compounds with their RP values are shown in the Supporting Information (Table S1).

Molecular Docking.

Throughout this paper we used the Ballesteros-Weinstein GPCR residue indexing system.⁴⁹ The molecular model of the A_{2B} AR^{15,16} was used in the ligand docking studies. All 72 compounds included in the DS, as well as compounds **7–10** synthesized in the present study, were docked to the A_{2B} AR and subjected to the MCM conformational search analysis as

recently described.¹⁶ MacroModel software was used in the automated docking studies.³³ The initial position of the receptor was the same for each compound.

CoMFA and CoMSIA Models.

The CoMFA and CoMSIA models were built using the Sybyl 7.3 software.⁴³ The Gasteiger-Hückel charges were assigned to each compound. In addition, the AM1, PM3, and MNDO partial atomic charges were calculated for each compound in the DS using MOE software.⁵² The conformations of the A_{2B} AR agonists obtained after molecular docking were used. Since during the molecular docking studies the receptor position was the same for each compound, additional alignment of the structures was not performed. The individual CoMFA and CoMSIA models, as well as combined CoMFA/CoMSIA models, were built. The both steric and electrostatic contours were calculated for CoMFA and the steric, electrostatic, H-bond donor and acceptor, and hydrophobic contours for CoMSIA were used. The four types of atomic charges mentioned above and the lattice space of 2 or 1 Å were examined in each model. All other parameters were set to their default values. The final model 3 was derived with the attenuation factor of $\alpha=0.5$ instead of its default value of R) 0.3. The Use SAMPLS option was deselected, and the value of the column filtering option was set to 2.0. The automatically determined optimal number of PLS components was used.

Chemical Synthesis. Materials and Instrumentation.

Anhydrous hydrazine, 2-furoic acid, benzotriazol-1-yloxytripyrrolidinophosphonium hexafluorophosphate (PyBop), diisopropylethylamine (DIPEA), and other reagents and solvents were purchased from Sigma-Aldrich (St. Louis, MO). 2-(4-Aminophenoxy)-*N*-phenylacetamide **78** was prepared as reported.²⁶

¹H NMR spectra were obtained with a Varian Gemini 300 spectrometer using CDCl₃ and CD₃OD as solvents. Chemical shifts are expressed in δ values (ppm) with tetramethylsilane (δ 0.00) for CDCl₃ and water (δ 3.30) for CD₃OD.

TLC analysis was carried out on aluminum sheets precoated with silica gel F₂₅₄ (0.2 mm) from Aldrich. Low-resolution mass spectrometry was performed with a JEOL SX102 spectrometer with 6 kV Xe atoms following desorption from a glycerol matrix or on an Agilent LC/MS 1100 MSD, with a Waters (Milford, MA) Atlantis C18 column. High-resolution mass spectroscopic (HRMS) measurements were performed on a proteomics optimized Q-TOF-2 (Micromass-Waters) using external calibration with polyalanine. Observed mass accuracies are those expected on the basis of the known performance of the instrument as well as trends in masses of standard compounds observed at intervals during the series of measurements. Reported masses are observed masses uncorrected for this time-dependent drift in mass accuracy.

2-(3''-(6''-Bromoindolyl)ethoxy)-6-hydrazinoadenosine (7).

A solution of 2-(3''-(5''-(bromo-1''-(*p*-toluenesulfonyl)indolyl)ethoxy)-6-chloro-3',4',5'-triacetyladenosine, **77** (24.0 mg, 0.030 mmol)¹⁶ was stirred with 0.50 mL of anhydrous hydrazine in a sealed flask. The reaction mixture was stirred at room temperature for 48 h. The solvent was evaporated under a vacuum, and the crude residue was subjected to

preparative TLC developed with a mixture of chloroform and methanol (8:2) to give **7** (7 mg, 43% yield). $^1\text{H NMR}$ (CD_3OD) δ 8.15 (1H, s), 7.50 (1H, d, J 8.5 Hz), 7.46 (1H, d, J 1.5 Hz), 7.18 (1H, s), 7.14 (1H, dd, J 1.5 and 8.5 Hz), 5.90 (1H, d, J 5.7 Hz), 4.70 (1H, t, J 5.0 Hz), 4.65 (2H, t, J 7.0 Hz), 4.35 (1H, dd, J 3.1 Hz and 5.2 Hz), 4.11 (1H, q, J 3.0), 3.85 (1H, dd, J 3.1 Hz and 12.5 Hz), 3.75 (1H, dd, J 3.1 Hz and 12.5 Hz), 3.21 (2H, t, J 7.0 Hz); HRMS (ESI MS m/z) calcd for $\text{C}_9\text{H}_{12}\text{BrN}_7\text{O}_5$ ($M - \text{H}$) 518.0788, found 518.0794.

2-(3''-(6''-Bromoindolyl)ethyloxy)-6-(*N*-furan-2-carbonyl)hydrazinoadenosine (**8**).

A solution of 2-furoic acid (11.2 mg, 0.10 mmol), PyBop (104 mg, 0.20 mmol), DIPEA (70.0 μL , 0.4 mmol) and 2.50 mL of anhydrous DMF was stirred at room temperature under N_2 for 30 min. Then 250 μL of the mixture was added to a stirring solution of **7** (3.0 mg, 0.005 mmol) and 250 μL of anhydrous DMF. The reaction mixture was stirred at room temperature for 18 h. The solvent was evaporated under vacuum, and the crude residue was subjected to preparative TLC developed with a mixture of chloroform and methanol (8:2) to give **8** (2 mg, 60% yield). $^1\text{H NMR}$ (CD_3OD) δ 8.20 (1H, s), 7.47 (1H, d, J 1.5 Hz), 7.42 (1H, d, J 8.5 Hz), 7.18 (1H, s), 7.06 (1H, dd, J 1.5 and 8.5 Hz), 7.01 (1H, m), 6.54 (1H, m), 6.32 (1H, m), 5.90 (1H, d, J 5.7 Hz), 4.70 (1H, t, J 5.0 Hz), 4.65 (2H, t, J 7.0 Hz), 4.35 (1H, dd, J 3.1 Hz and 5.2 Hz), 4.11 (1H, q, J 3.0), 3.85 (1H, dd, J 3.1 Hz and 12.5 Hz), 3.75 (1H, dd, J 3.1 Hz and 12.5 Hz), 3.21 (2H, t, J 7.0 Hz); HRMS (ESI MS m/z) calcd for $\text{C}_{25}\text{H}_{25}\text{BrN}_7\text{O}_7$ ($M + \text{H}$) 614.0999, found 614.0981.

2-(3''-(6''-Bromo-1''-(*p*-toluenesulfonyl)indolyl)ethyloxy)-6-(4-((phenylcarbamoyl)methoxy)phenylamino)-3',4',5'-triacetyladenosine (**79**).

A solution of 2-(3''-(5''-(bromo-1''-(*p*-toluenesulfonyl)indolyl)ethyloxy)-6-chloro-3',4',5'-triacetyladenosine, **77** (24.0 mg, 0.030 mmol), was dissolved in 1.0 mL of anhydrous ethanol. 2-(4-Aminophenoxy)-*N*-phenylacetamide **78** (8.0 mg, 0.033 mmol) and 5.0 μL of triethylamine (TEA) were added. The flask was then sealed and heated to 110°C for 18 h. The solvent was evaporated under a vacuum, and the crude residue was subjected to preparative TLC developed with a mixture of toluene and acetone (1:1) to give **79** (16 mg, 50% yield). $^1\text{H NMR}$ (CDCl_3) δ 7.81 (1H, s), 7.72 (2H, d, J 8.2 Hz), 7.69 (2H, d, J 8.2 Hz), 7.60 (2H, d, J 9.0 Hz), 7.45 (2H, d, J 9.0 Hz), 7.35 (1H, t, 8.2 Hz), 7.12 (1H, s), 7.08 (1H, dd, J 1.5 and 8.5 Hz), 7.02 (d, 2H, J 9.0 Hz), 6.11 (1H, d, J 5.7 Hz), 5.96 (1H, t, J 5.0 Hz), 5.52 (1H, t, J 7.0 Hz), 4.62 (2H, s), 4.33 (1H, dd, J 3.1 Hz and 5.2 Hz), 3.20 (2H, t, J 7.0 Hz), 2.31 (3H, s), 2.13 (3H, s), 2.08 (3H, s), 2.06 (3H, s). HRMS (ESI MS m/z) calcd for $\text{C}_{47}\text{H}_{44}\text{BrN}_7\text{O}_{12}\text{S}$ ($M + \text{H}$)⁺ 1010.8609, found 1010.8622.

2-(3''-(6''-Bromo-1''-*N*-indolyl)ethyloxy)-6-(4-carboxymethoxy)phenylamino)-3',4',5'-triacetyladenosine (**80**).

Compound **79** (16 mg, 0.015 mmol) was stirred with 1.0 mL of 0.25 M KOH in MeOH. The reaction mixture was stirred under N_2 at room temperature for 18 h. The solvent was evaporated under a vacuum, and the crude residue was subjected to preparative TLC developed with a mixture of chloroform and methanol (4:1) to give **80** (7 mg, 51% yield). $^1\text{H NMR}$ (CD_3OD) δ 7.78 (2H, d, J 8.2 Hz), 7.72 (2H, d, J 8.2 Hz), 7.68 (2H, d, J 9.0 Hz), 7.62 (2H, d, J 9.0 Hz), 7.35 (1H, t, 8.2 Hz), 7.12 (1H, s), 7.08 (1H, dd, J 1.5 and 8.5 Hz),

6.95(d, 2H, *J* 9.0 Hz), 5.90 (1H, d, *J* 5.7 Hz), 4.74 (1H, t, *J* 5.0 Hz), 4.65, (1H, S), 4.60 (2H, t, *J* 7.0 Hz), 4.33 (1H, dd, *J* 3.1 and 5.2 Hz), 4.15 (1H, q, *J* 3.0), 3.85 (1H, dd, *J* 3.1 and 12.5 Hz), 3.75 (1H, dd, *J* 3.1 and 12.5 Hz), 3.65 (1H, s), 3.20 (2H, t, *J* 7.0 Hz); LRMS (ESI MS *m/z*) calcd for C₂₈H₂₆BrN₆O₈ (M - H)⁻ 653.1, found 653.1.

2-(3''-(6''-Bromo-1''-*N*-indolyl)ethyloxy)-6-(4-((phenylcarbamoyl)methoxy)phenylamino)adenosine (9) and 2-(3''-(6''-Bromo-1''-*N*-indolyl)ethyloxy)-6-(4-((*N*-pyrrolidinecarbamoyl)methoxy) phenylamino)adenosine (10).

A solution of **80** (5.0 mg, 0.007 mmol), PyBop (8.0 mg, 0.015 mmol), and DIPEA (5.4 μ L, 0.030 mmol) in 0.500 mL of anhydrous DMF was stirred at room temperature under N₂ for 30 min. Aniline (5.0 μ L, 0.050 mmol) was added to the reaction mixture, and stirring continued at room temperature for 18 h. The solvent was evaporated under a vacuum, and the crude residue was subjected to preparative TLC developed with a mixture of chloroform and methanol (9:1) to give **9** (2 mg, 40% yield). ¹H NMR (CD₃OD) δ 8.16 (1H, s), 7.82 (2H, d, *J* 8.2 Hz), 7.72(2H, d, *J* 8.2 Hz), 7.68 (2H, d, *J* 9.0 Hz), 7.62 (2H, d, *J* 9.0 Hz), 7.35 (1H, t, 8.2 Hz), 7.12 (1H, s), 7.08 (1H, dd, *J* 1.5 and 8.5 Hz), 6.95(d, 2H, *J* 9.0 Hz), 5.90 (1H, d, *J* 5.7 Hz), 4.74 (1H, t, *J* 5.0 Hz), 4.65, (1H, S), 4.60 (2H, t, *J* 7.0 Hz), 4.33 (1H, dd, *J* 3.1 and 5.2 Hz), 4.15 (1H, q, *J*3.0), 3.85 (1H, dd, *J* 3.1 and 12.5 Hz), 3.75 (1H, dd, *J* 3.1 and 12.5 Hz), 3.65 (1H, s), 3.20 (2H, t, *J* 7.0 Hz); HRMS (ESI MS *m/z*) calcd for C₃₄H₃₂BrN₇O₇ (M + H)⁺ 730.1625, found 730.1663.

Compound **10** was also isolated from the preparative TLC, (1.0 mg, 18% yield). ¹H NMR (CD₃OD) δ 8.16 (1H, s), 7.82 (2H, d, *J* 8.2 Hz), 7.72(2H, d, *J* 8.2 Hz), 7.68 (2H, d, *J* 9.0 Hz), 7.62 (2H, d, *J* 9.0 Hz), 7.35 (1H, t, 8.2 Hz), 7.12 (1H, s), 7.08 (1H, dd, *J* 1.5 and 8.5 Hz), 6.95(d, 2H, *J* 9.0 Hz), 5.90 (1H, d, *J* 5.7 Hz), 4.74 (1H, t, *J* 5.0 Hz), 4.65, (1H, S), 4.60 (2H, t, *J* 7.0 Hz), 4.33 (1H, dd, *J* 3.1 and 5.2 Hz), 4.15 (1H, q, *J*3.0), 3.85 (1H, dd, *J* 3.1 and 12.5 Hz), 3.75 (1H, dd, *J* 3.1 and 12.5 Hz), 3.65 (1H, s), 3.52 (2H, m), 3.20 (2H, t, *J* 7.0 Hz), 2.02 (1H, m), 1.90 (1H, m); HRMS (ESI MS *m/z*) calcd for C₃₂H₃₅BrN₇O₇ (M + H)⁺ 708.1781, found 708.1775.

HPLC Analysis of Compounds 7–10.

The purity of the nucleoside products was demonstrated by HPLC as in our previous study,¹⁶ using an Agilent 1100 series HPLC (Santa Clara, CA) equipped with a Phenomenex Luna 5 μ m C18(2) 100A analytical column (250 mm \times 10 mm; Torrance, CA). All compounds were tested with a flow rate of 2 mL/min and the following acetonitrile/water linear gradient: 0 min, 20% acetonitrile; 20 min, 80% acetonitrile. Peaks were detected by UV absorption using a diode array detector. All compounds were found to be >98% pure by HPLC analysis. The compounds eluted at the following retention times: **7**, 9.9 min; **8**, 8.1 min; **9**, 10.0 min; **10**, 9.9 min.

Pharmacological Methods. Binding Assay.

Competitive radioligand binding assays were performed as described previously.⁵⁰ [³H]CCPA (2-chloro-*N*⁶-cyclopentyladenosine, 42.6 Ci/mmol) and [³H]CGS21680 (2-[*p*-(2-carboxyethyl)phenylethylamino]-5'-*N*-ethylcarboxamidoadenosine, 40.5 Ci/mmol) were purchased from Perkin-Elmer (Waltham, MA). Human A₁ ARs were stably expressed in

Chinese hamster ovary (CHO) cells, while the human A_{2A} AR was stably expressed in HEK293 cells. Cell membrane suspensions were prepared as described.⁵¹ For the binding determination, each tube contained 50 μ L of the appropriate radioligand (A₁[³H]CCPA, final concentration of 1.0 nM; A_{2A} [³H]CGS21680, final concentration of 10 nM), 50 μ L of increasing concentrations of the compounds, and 100 μ L of cell membrane suspension expressing the appropriate receptor diluted with Tris-HCl buffer (50 mM, pH 7.4) containing 10 mM MgCl₂. Nonspecific binding was determined using 10 μ M NECA. The tubes were incubated at 25 °C for 1 h and then filtered through Whatman GF/B filters under reduced pressure using an MT-24 cell harvester (Brandell; Gaithersburg, MD). Filters were washed rapidly three times with ice-cold buffer. After the filters were washed, they were placed in scintillation vials containing 5 mL of Hydrofluor scintillation buffer and counted using a Perkin-Elmer liquid scintillation analyzer. The K_i values were determined using Prism (GraphPad, San Diego, CA) for all assays.

cAMP Assay.

cAMP was measured in CHO cells stably expressing the human A_{2A} AR.⁵¹ cAMP accumulation was measured with cAMP enzyme immunoassay kit according to the instructions in the assay manual (Sigma; St. Louis, MO).

Supplementary Material

Refer to Web version on PubMed Central for supplementary material.

Acknowledgment.

We thank Dr. John Lloyd (NIDDK) for mass spectral determinations. This research was supported by the Intramural Research Program of the NIH, National Institute of Diabetes and Digestive and Kidney Diseases. We thank Dr. Stefano Costanzi (NIDDK) for helpful discussions.

References

- (1). Jacobson KA; Gao Z-G Adenosine receptors as therapeutic targets. *Nat. Rev. Drug. Discov* 2006, 5, 247–264. [PubMed: 16518376]
- (2). Burnstock G Purine and pyrimidine receptors. *Cell. Mol. Life Sci* 2007, 64, 1471–1483. [PubMed: 17375261]
- (3). Gao Z-G; Jacobson KA Emerging adenosine receptor agonists. *Expert Opin. Emerging Drugs* 2007, 12, 479–492.
- (4). Eckle T; Krahn T; Grenz A; Köhler D; Mittelbronn M; Ledent C; Jacobson MA; Osswald H; Thompson LF; Unertl K; Eltzhig HK Cardioprotection by ecto-5'-nucleotidase (CD73) and A_{2B} adenosine receptors. *Circulation* 2007, 115, 1581–1590. [PubMed: 17353435]
- (5). Németh ZH; Bleich D; Csóka B; Pacher P; Mabley JG; Himer L; Vizi ES; Deitch EA; Szabó C; Cronstein BN; Haskó G Adenosine receptor activation ameliorates type 1 diabetes. *FASEB J.* 2007, 10, 2379–2388.
- (6). Sum CS; Tikhonova IG; Neumann S; Engel S; Raaka BM; Costanzi S; Gershengorn MC Identification of residues important for agonist recognition and activation in GPR40. *J. Biol. Chem* 2007, 282, 29248–29255. [PubMed: 17699519]
- (7). Ivanov AA; Voronkov AE; Baskin II; Palyulin VA; Zefirov NS The study of the mechanism of binding of human ML1A melatonin receptor ligands using molecular modeling. *Dokl. Biochem. Biophys* 2004, 394, 49–52. [PubMed: 15116569]

- (8). Li JH; Han S-J; Hamdan FF; Kim S-K; Jacobson KA; Bloodworth LM; Zhang X; Wess J Distinct structural changes in a G protein-coupled receptor caused by different classes of agonist ligands. *J. Biol. Chem* 2007, 282, 26284–26293. [PubMed: 17623649]
- (9). Rodina EV; Vorobyeva NN; Kurilova SA; Belenikin MS; Fedorova NV; Nazarova TI ATP as effector of inorganic pyrophosphatase of *Escherichia coli*. Identification of the binding site for ATP. *Biochemistry (Moscow)* 2007, 72, 93–99. [PubMed: 17309442]
- (10). Ivanov AA; Baskin II; Palyulin VA; Piccagli L; Baraldi PG; Zefirov NS Molecular modeling and molecular dynamics simulation of the human A_{2B} adenosine receptor. The study of the possible binding modes of the A_{2B} receptor antagonists. *J. Med. Chem* 2005, 48, 6813–6820. [PubMed: 16250640]
- (11). Ferretti V; Bertoni E A preliminary docking study of a potent and selective xanthinic antagonist to the adenosinic A_{2B} receptor. *MinerVaBiotechnol.* 2005, 16, 79–83.
- (12). Kim SK; Gao Z-G; Jeong LS; Jacobson KA Docking studies of agonists and antagonists suggest an activation pathway of the A₃ adenosine receptor. *J. Mol. Graphics Modell* 2006, 25, 562–577.
- (13). Colotta V; Catarzi D; Varano F; Capelli F; Lenzi O; Filacchioni G; Martini C; Trincavelli L; Ciampi O; Pugliese AM; Pedata F; Schiesaro A; Morizzo E; Moro S New 2-arylpyrazolo[3,4-c]quinoline derivatives as potent and selective human A₃ adenosine receptor antagonists. Synthesis, pharmacological evaluation, and ligand-receptor modeling studies. *J. Med. Chem* 2007, 50, 4061–4074. [PubMed: 17665891]
- (14). Palaniappan KK; Gao Z-G; Ivanov AA; Greaves R; Adachi H; Besada P; Kim HO; Kim AY; Choe AA; Jeong LS; Jacobson KA Probing the binding site of the A₁ adenosine receptor reengineered for orthogonal recognition by tailored nucleosides. *Biochemistry* 2007, 46, 7437–7448. [PubMed: 17542617]
- (15). Ivanov AA; Palyulin VA; Zefirov NS Computer aided comparative analysis of the binding modes of the adenosine receptor agonists for all known subtypes of adenosine receptors. *J. Mol. Graphics Modell* 2007, 25, 740–754.
- (16). Adachi H; Palaniappan KK; Ivanov AA; Bergman N; Gao Z-G; Jacobson KA Structure-activity relationships of 2, N⁶, 5'-substituted adenosine derivatives with potent activity at the A_{2B} adenosine receptor. *J. Med. Chem* 2007, 50, 1810–1827. [PubMed: 17378544]
- (17). Loging W; Harland L; Williams-Jones B High-throughput electronic biology: mining information for drug discovery. *Nature ReV. Drug DiscoVery* 2007, 6, 220–230. [PubMed: 17330071]
- (18). Muegge I; Oloff S Advances in virtual screening. *Drug DiscoVery Today* 2006, 3, 405–411.
- (19). Akamatsu M Current state and perspectives of 3D-QSAR. *Curr. Top. Med. Chem* 2002, 2, 1381–1394. [PubMed: 12470286]
- (20). Tchilibon S; Kim SK; Gao ZG; Harris BA; Blaustein J; Gross AS; Melman N; Jacobson KA Exploring distal regions of the A₃ adenosine receptor binding site: sterically-constrained N⁶-(2-phenylethyl)adenosine derivatives as potent ligands. *Bioorg. Med. Chem* 2004, 12, 2021–2034. [PubMed: 15080906]
- (21). Li A-H; Moro S; Melman N; Ji X.-d.; Jacobson KA Structure activity relationships and molecular modeling of 3,5-diacyl-2,4-dialkylpyridine derivatives as selective A₃ adenosine receptor antagonists. *J. Med. Chem* 1998, 41, 3186–3201. [PubMed: 9703464]
- (22). Moro S; Braiuca P; Deflorian F; Ferrari C; Pastorin G; Cacciari B; Baraldi PG; Varani K; Borea PA; Spalluto G Combined target-based and ligand-based drug design approach as a tool to define a novel 3D-pharmacophore model of human A₃ adenosine receptor antagonists: pyrazolo[4,3-e]1,2,4-triazolo[1,5-c]pyrimidine derivatives as a key study. *J. Med. Chem* 2005, 48, 152–162. [PubMed: 15634009]
- (23). Rieger JM; Brown ML; Sullivan GW; Linden J; Macdonald TL Design, synthesis, and evaluation of novel A_{2A} adenosine receptor agonists. *J. Med. Chem* 2001, 44, 531–539. [PubMed: 11170643]
- (24). Fossa P; Pestarino M; Menozzi G; Mosti L; Schenone S; Ranise A; Bondavalli F; Trincavelli ML; Lucacchini A; Martini C New pyrazolo[3,4-b]pyridones as selective A₁ adenosine receptor antagonists: synthesis, biological evaluation and molecular modelling studies. *Org. Biomol. Chem* 2005, 3, 2262–2270. [PubMed: 16010360]

- (25). Baraldi PG; Preti D; Tabrizi MA; Fruttarolo F; Romagnoli R; Carrion MD; Cara LCL; Moorman AR; Varani K; Borea PA Synthesis and biological evaluation of novel 1-deoxy-1-[6-[(hetero)arylcarbonyl]hydrazine]-9H-purin-9-yl]-N-ethyl--D-ribofuranuronamide derivatives as useful templates for the development of A2B adenosine receptor agonists. *J. Med. Chem* 2007, 50, 374–380. [PubMed: 17228880]
- (26). Baraldi PG; Preti D; Tabrizi MA; Fruttarolo F; Saponaro G; Baraldi S; Romagnoli R; Moorman AR; Gessi S; Varani K; Borea PA N6-[(Hetero)aryl(cyclo)alkyl-carbamoyl-methoxy-phenyl]-(2-chloro)-5'-N-ethylcarboxamido-adenosines: the first example of adenosine-related structures with potent agonist activity at the human A_{2B} adenosine receptor. *Bioorg. Med. Chem* 2007, 15, 2514–2527. [PubMed: 17306548]
- (27). Dooley MJ; Quinn RJ The three binding domain model of adenosine receptors: molecular modeling aspects. *J. Med. Chem* 1992, 35, 211–216. [PubMed: 1732538]
- (28). Elzein E; Palle V; Wu Y; Maa T; Zeng D; Zablocki J 2-Pyrazolyl-N⁶-substituted adenosine derivatives as high affinity and selective adenosine A₃ receptor agonists. *J. Med. Chem* 2004, 47, 4766–4773. [PubMed: 15341491]
- (29). Okada T; Sugihara M; Bondar A-N; Elstner M; Entel P; Buss V The retinal conformation and its environment in rhodopsin in light of new 2.2 Å crystal structure. *J. Mol. Biol* 2004, 342, 571–583. [PubMed: 15327956]
- (30). Lodowski DT; Salom D; Le Trong I; Teller DC; Ballesteros JA; Palczewski K; Stenkamp RE Crystal packing analysis of rhodopsin crystals. *J. Struct. Biol* 2007, 158, 455–462. [PubMed: 17374491]
- (31). Schueler-Furman O; Wang C; Bradley P; Misura K; Baker D Progress in modeling of protein structures and interactions. *Science* 2005, 310, 638–642. [PubMed: 16254179]
- (32). Fanelli F; De Benedetti PG Computational modeling approaches to structure-function analysis of G protein-coupled receptors. *Chem. Rev* 2005, 105, 3297–3351. [PubMed: 16159154]
- (33). Mohamadi FN; Richards GJ; Guida WC; Liskamp R; Lipton M; Caufield C; Chang G; Hendrickson T; Still WC Macro-Models an integrated software system for modeling organic and bioorganic molecules using molecular mechanics. *J. Comput. Chem* 1990, 11, 440–467.
- (34). Costanzi S; Ivanov AA; Tikhonova IG; Jacobson KA Structure and function of G protein-coupled receptors studied using sequence analysis molecular modeling and receptor engineering: adenosine receptors. *Front. Drug Des. DiscoVery* 2007, 3, 63–79.
- (35). Ivanova AA; Ivanov AA; Oliferenko AA; Palyulin VA; Zefirov NS Highly diverse, massive organic data as explored by a composite QSPR strategy: an advanced study of boiling point. *SAR QSAR EnViron. Res* 2005, 16, 231–246. [PubMed: 15804811]
- (36). Kim SK; Jacobson KA Three-dimensional quantitative structure-activity relationship of nucleosides acting at the A₃ adenosine receptor: analysis of binding and relative efficacy. *J. Chem. Inf. Model* 2007, 47, 1225–1233. [PubMed: 17338510]
- (37). Moro S; Bacilieri M; Ferrari C; Spalluto G Autocorrelation of molecular electrostatic potential surface properties combined with partial least squares analysis as alternative attractive tool to generate ligand-based 3D QSARs. *Curr. Drug DiscoVery Technol* 2005, 2, 13–21.
- (38). Li A-H; Moro S; Forsyth N; Melman N; Ji X; Jacobson KA Synthesis, CoMFA analysis, and receptor docking of 3,5-diacyl-2,4-dialkylpyridine derivatives as selective A₃ adenosine receptor antagonists. *J. Med. Chem* 1999, 42, 706–721. [PubMed: 10052977]
- (39). Palyulin VA; Radchenko VA; Zefirov NS Molecular field topology analysis method in QSAR studies of organic compounds. *J. Chem. Inf. Comput. Sci* 2000, 40, 659–667. [PubMed: 10850771]
- (40). Costanzi S; Tikhonova IG; Ohno M; Joshi BV; Colson AO; Houston D; Maddileti S; Harden TK; Jacobson KA P2Y₁ antagonists: combining receptor-based modeling and QSAR for a quantitative prediction of the biological activity based on consensus scoring. *J. Med. Chem* 2007, 50, 3229–3241. [PubMed: 17564423]
- (41). Drabczy ska A; Müller CE; Schiedel A; Schumacher B; Karolak-Wojciechowska J; Fruzi ski A; Zobnina W; Yuzlenko O; Kie -Kononowicz K Phenylethyl-substituted pyrimido[2,1-f]purinediones and related compounds: structure-activity relationships as adenosine A₁ and A_{2A} receptor ligands. *Bioorg. Med. Chem* 2007, 15, 6956–6974. [PubMed: 17827019]

- (42). Tikhonova IG; Baskin II; Palyulin VA; Zefirov NS CoMFA and homology-based models of the glycine binding site of *N*-methyl-D-aspartate receptor. *J. Med. Chem* 2003, 46, 1609–1616. [PubMed: 12699379]
- (43). SYBYL, version 7.3; Tripos Inc. (1699 South Hanley Road, St. Louis, MO 63144).
- (44). Klebe G; Abraham U; Mietzner T Molecular similarity indices in a comparative analysis (CoMSIA) of drug molecules to correlate and predict their biological activity. *J. Med. Chem* 1994, 37, 4130–4146. [PubMed: 7990113]
- (45). San Juan AA Structural investigation of PAP derivatives by CoMFA and CoMSIA reveals novel insight towards inhibition of Bcr-Abl oncoprotein. *J. Mol. Graphics Modell* 2007, 26, 482–493.
- (46). de Zwart M; Link R; von Frijtag Drabbe Künzel JK; Cristalli G; Jacobson KA; Townsend-Nicholson A; IJzerman AP Nucleosides Nucleotides 1998, 17, 969–985. [PubMed: 9708319]
- (47). Vittori S; Costanzi S; Lambertucci C; Portino FR; Taffi S; Volpini R; Klotz K-N; Cristalli G A2B adenosine receptor agonists: synthesis and biological evaluation of 2-phenylhydroxypropynyl adenosine and NECA derivatives. *Nucleosides, Nucleotides Nucleic Acids* 2004, 23, 471–481. [PubMed: 15043167]
- (48). Volpini R; Costanzi S; Lambertucci C; Taffi S; Vittori S; Klotz K-N; Cristalli G *N*⁶-Alkyl-2-alkynyl derivatives of adenosine as potent and selective agonists at the human adenosine A₃ receptor and a starting point for searching A_{2B} ligands. *J. Med. Chem* 2002, 45, 3271–3279. [PubMed: 12109910]
- (49). Ballesteros J; Weinstein H Integrated methods for the construction of three-dimensional models of structure-function relations in G protein-coupled receptors. *Methods Neurosci.* 1995, 25, 366–428.
- (50). Perreira M; Jiang JK; Klutz AM; Gao ZG; Shainberg A; Lu C; Thomas CJ; Jacobson KA “Reversine” and its 2-substituted adenine derivatives as potent and selective A₃ adenosine receptor antagonists. *J. Med. Chem* 2005, 48, 4910–4918. [PubMed: 16033270]
- (51). Gao ZG; Mamedova LM; Chen P; Jacobson KA 2-Substituted adenosine derivatives: affinity and efficacy at four subtypes of human adenosine receptors. *Biochem. Pharmacol* 2004, 68, 1985–1993. [PubMed: 15476669]
- (52). Molecular Operating Environment, version 2008.05; Chemical Computing Group: Montreal, Canada.
- (53). Rosenbaum DM; Cherezov V; Hanson MA; Rasmussen SGF; Thian FS; Kobilka TS; Choi HJ; Yao XJ; Weis WI; Stevens RC; Kobilka BK GPCR engineering yields high-resolution structural insights into α_2 adrenergic receptor function. *Science* 2007, 318, 1266–1273. [PubMed: 17962519]

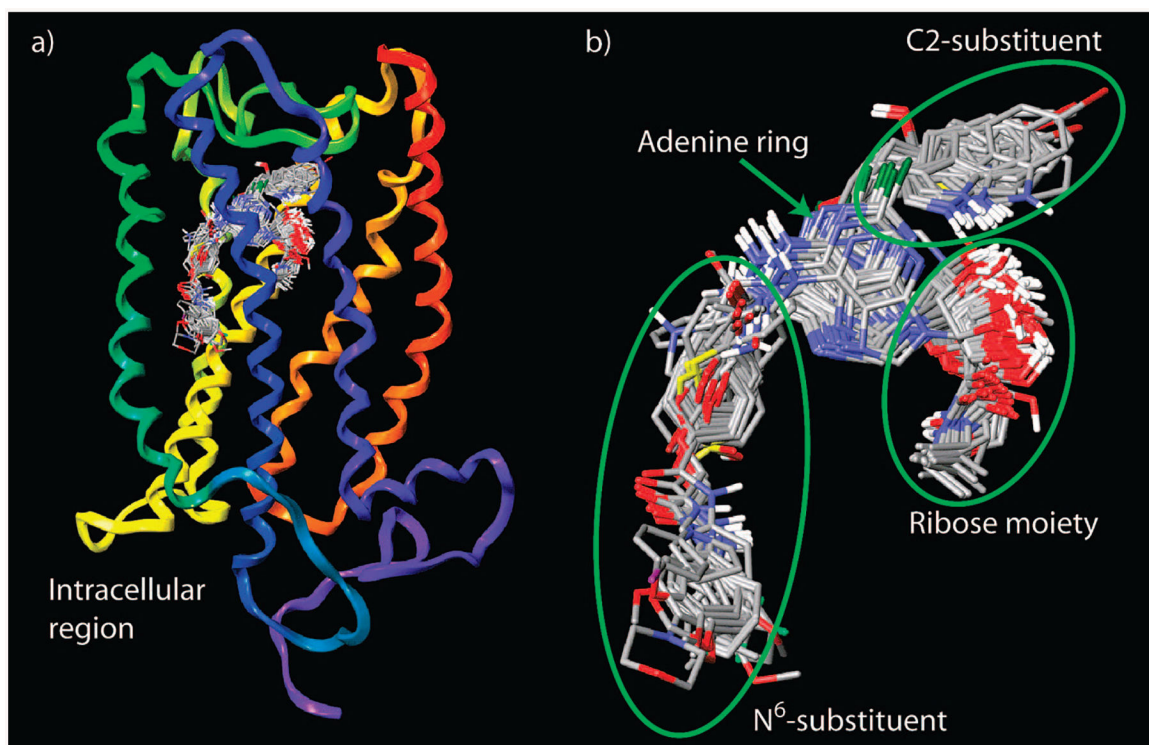


Figure 1.

(a) Overlay of all docked ligands at the A_{2B} AR. (b) Structural alignment of the ligands extracted from the ligand–receptor models. The structure of the A_{2B} AR is colored by residue position: N-terminus and TM1 in orange, TM2 in ochre, TM3 in yellow, TM4 in green, TM5 in cyan, TM6 in blue, TM7 and C-terminus in purple.

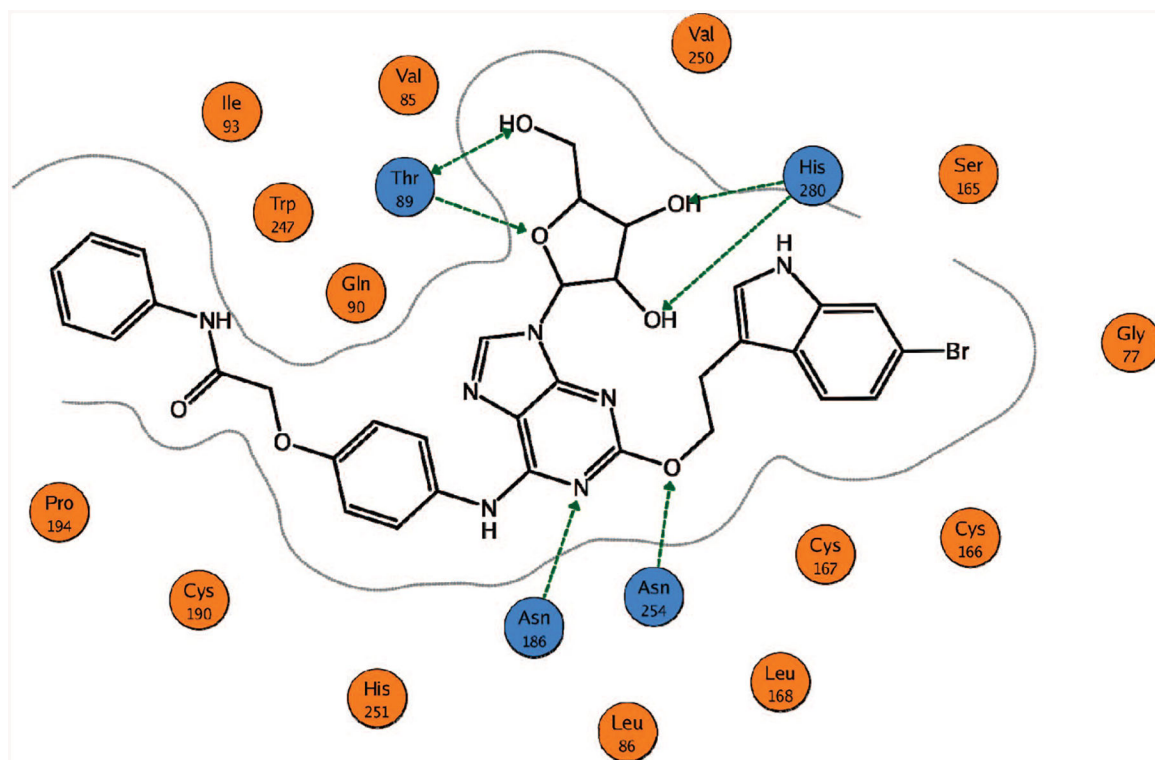


Figure 2. Schematic representation of the ligand binding mode obtained after the docking studies. The binding mode of the 5'-OH derivative **9** is shown as an example. The green arrows correspond to the putative H-bonds. The critical residues involved in interactions with a ligand are colored in blue. For 5'-uronamide derivatives, the carbonyl oxygen atom was H-bonded to Ser279^{7,42} (not shown).

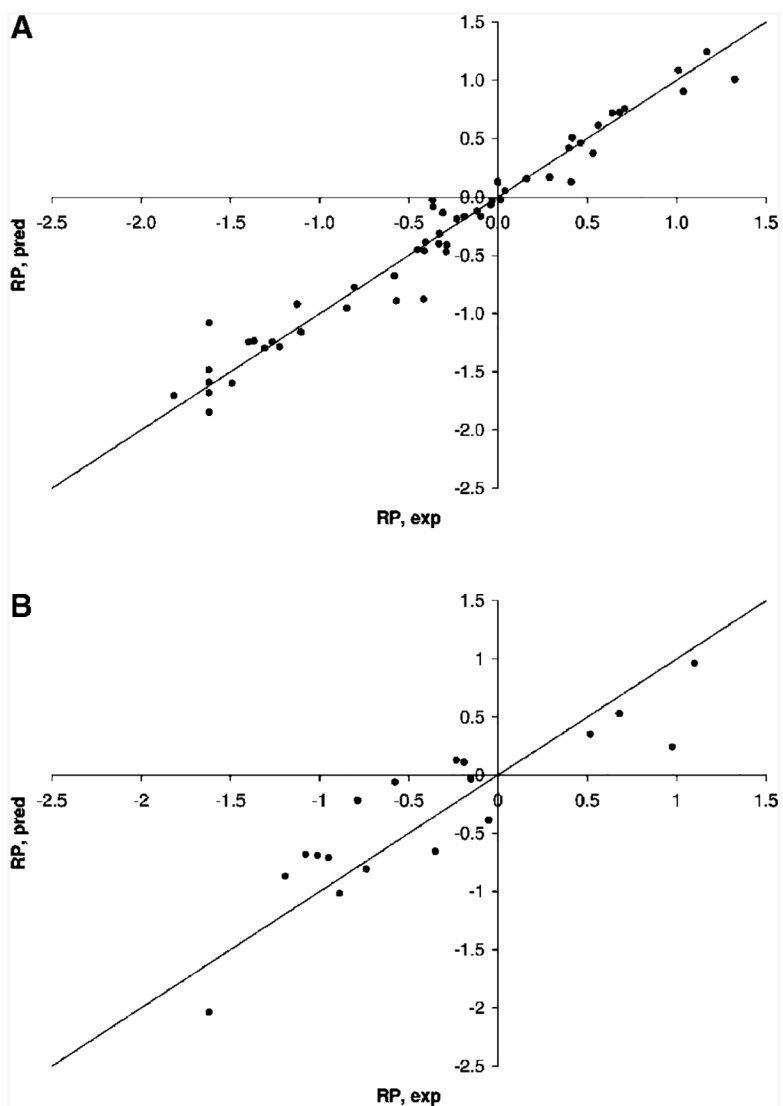


Figure 3. Correlation plots obtained for the training (A) and test (B) sets of compounds with the CoMFA/CoMSIA model 3.

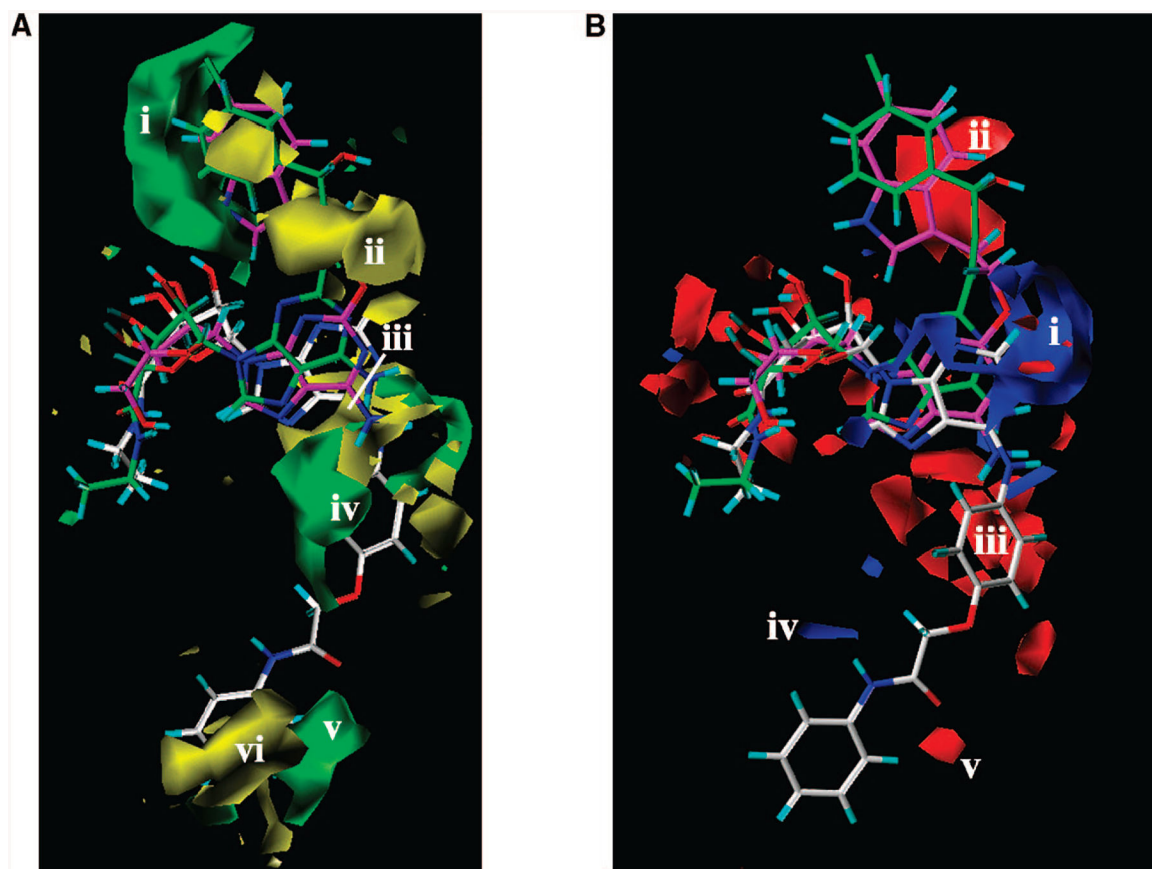


Figure 4.

Contour maps of the CoMFA regions are shown around (*S*)-PHPNECA **2** (carbon atoms colored in green), MRS3997 **4** (carbon atoms colored in magenta), and ligand **6** (carbon atoms colored in white) superimposed in their conformations obtained after the docking studies; regions i and ii surround the 2 substituent. (A) Contour maps of the CoMFA steric regions (green, favored; yellow, disfavored). Regions iii–vi surround the N^6 substituent, and regions i and ii are located around the C2 substituent. (B) Contour maps of the CoMFA electrostatic regions. Blue regions are favorable for more positively charged groups; red regions are favorable for less positively charged groups. Polyhedral regions labeled with Roman numerals are discussed in the text. Regions i and ii surround the C2 substituent, and regions iii–v surround the N^6 substituent.

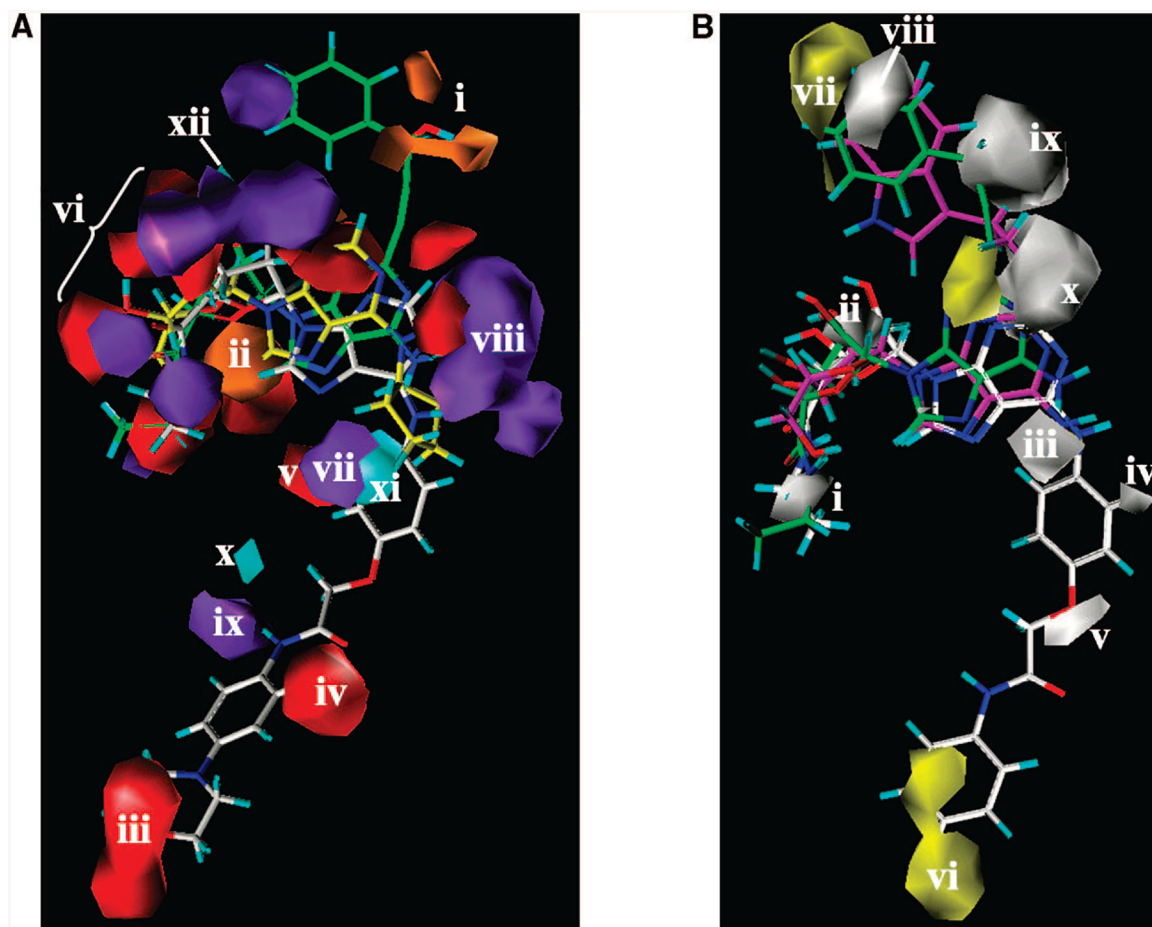
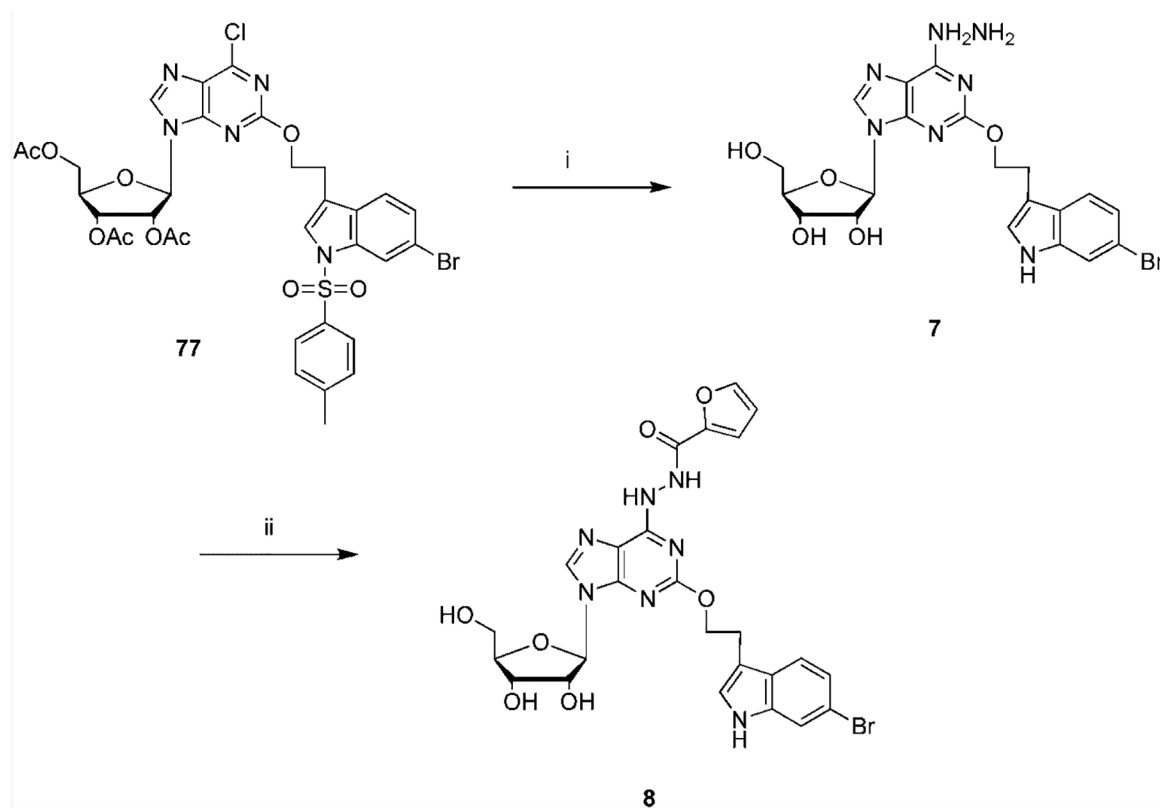
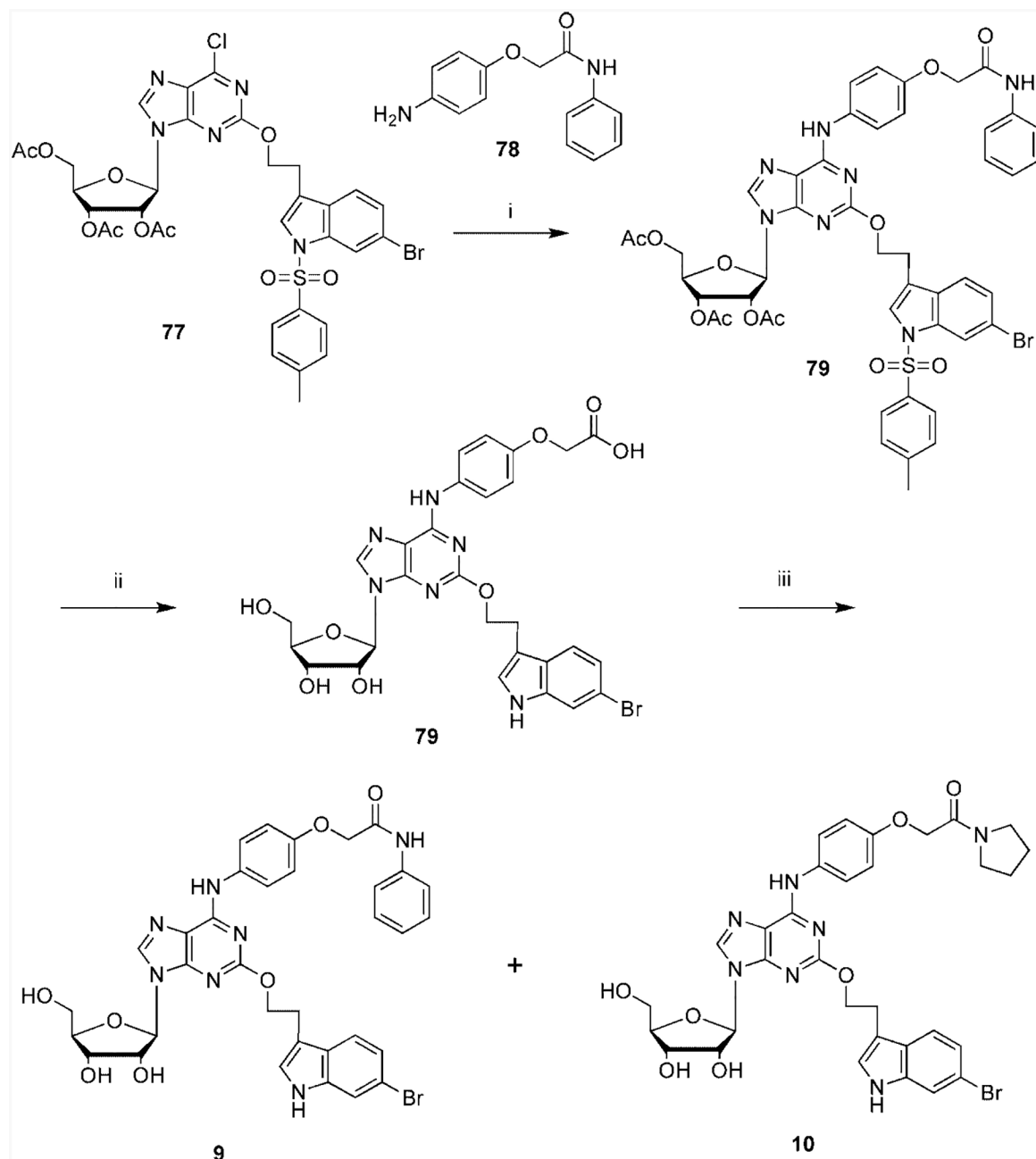


Figure 5.

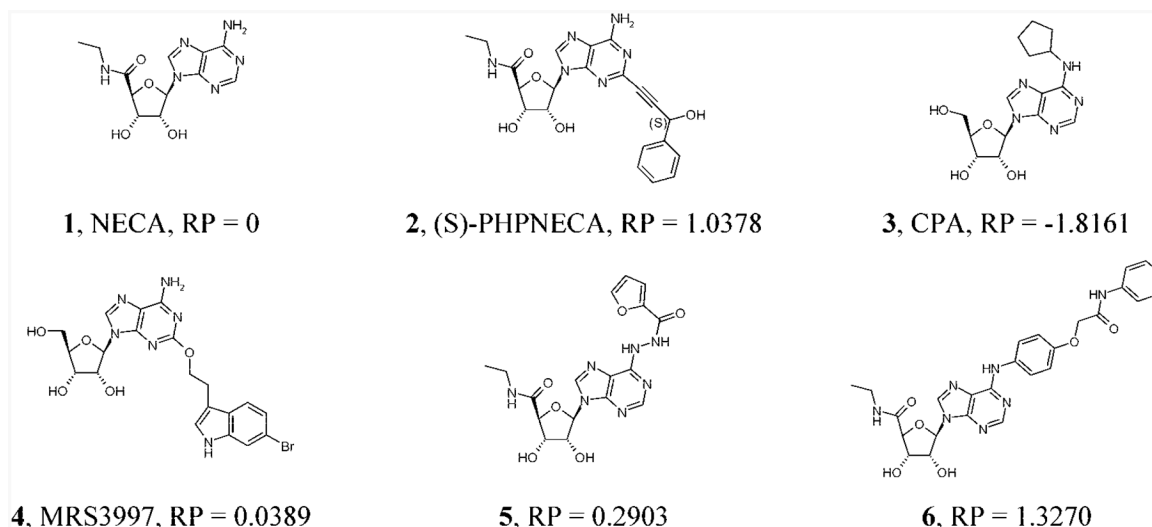
(A) Contour maps of the CoMSIA H-bond donor and acceptor regions are shown around (*S*)-PHPNECA **2** (carbon atoms colored in green), CPA **3** (carbon atoms colored in yellow), and ligand **68** (carbon atoms colored in white): cyan plots, regions favored for the receptor H-bond acceptor groups; purple, regions disfavored for the receptor H-bond acceptor groups; orange, regions favored for the receptor H-bond donating groups; red, regions disfavored for the receptor H-bond donating groups. Region i appeared in proximity to the hydroxyl group of the 2-(3-hydroxy-3-phenyl)propyn1-yl moiety of (*S*)-PHPNECA **2** and (*S*)-PHPAdo **33**. Region ii is located between the ribose oxygen atom and the 5'-OH group of the adenosine derivatives. Regions iii–v and vii–xi surround the N^6 substituent. The group of regions vi and xii surround the 2'- and 3'-hydroxyl groups of the ribose moiety. (B) Contour maps of the CoMSIA hydrophobic regions (yellow, favored; white, disfavored) are shown around (*S*)-PHPNECA **2** (carbon atoms colored in green), MRS3997 **4** (carbon atoms colored in magenta), and ligand **6** (carbon atoms colored in white) superimposed in their receptor-docked conformations. Polyhedral regions labeled with Roman numerals are discussed in the text. Region i corresponds to the 5'-position. Region ii is located in proximity to the 2'- and 3'-hydroxyl groups of the ribose moiety. Regions iii–visurround the N^6 substituent, and regions vii–x appear around the 2 substituent.

**Scheme 1.**

Synthetic Routes to the Novel 6-Hydrazinopurine-9-ribose Derivatives^{a a} Reagents: (i) hydrazine; (ii) furoic acid, PyBop, DIPEA, DMF.

**Scheme 2.**

Synthetic Routes to the Novel 6-Arylamino-purine-9-ribose Derivatives^{a a} Reagents and conditions: (i) EtOH, TEA, 110°, 18 h; (ii) KOH; (iii) aniline, PyBop, DIPEA, DMF.

**Chart 1.**

Structures of Known AR Agonists That Were Used as Reference Compounds at the A_{2B} AR^a RP: NECA related potency. RP = $pEC_{50}(\text{comp})_i - pEC_{50}(\text{NECA})_i$, where i represents the same reference publication.

Table 1.

Statistical Parameters of the CoMFA and CoMSIA Models^a

GH charge type	lattice space = 2 Å				lattice space = 1 Å	
	AM1 charge type	PM3 charge type	MNDO charge type	MNDO charge type	MNDO charge type	MNDO charge type
CoMFA						
$R^2 = 0.233$	$R^2 = 0.914$	$R^2 = 0.705$	$R^2 = 0.705$	$R^2 = 0.705$	$R^2 = 0.952$	
$Q^2 = 0.538$	$Q^2 = 0.585$	$Q^2 = 0.579$	$Q^2 = 0.492$	$Q^2 = 0.492$	$Q^2 = 0.525$	
SEE = 0.233	SEE = 0.252	SEE = 0.245	SEE = 0.458	SEE = 0.458	SEE = 0.193	
$F = 87$	$F = 102$	$F = 91$	$F = 40$	$F = 40$	$F = 129$	
$C = 7$	$C = 5$	$C = 6$	$C = 3$	$C = 3$	$C = 7$	
CoMSIA, ^b $\alpha = 0.30$						
$R^2 = 0.782$	$R^2 = 0.919$	$R^2 = 0.917$	$R^2 = 0.927$	$R^2 = 0.927$	$R^2 = 0.915$	
$Q^2 = 0.475$	$Q^2 = 0.605$	$Q^2 = 0.612$	$Q^2 = 0.571$	$Q^2 = 0.571$	$Q^2 = 0.589$	
SEE = 0.398	SEE = 0.250	SEE = 0.253	SEE = 0.237	SEE = 0.237	SEE = 0.253	
$F = 44$	$F = 75$	$F = 73$	$F = 84$	$F = 84$	$F = 84$	
$C = 4$	$C = 7$	$C = 7$	$C = 7$	$C = 7$	$C = 6$	
CoMFA and CoMSIA, ^b $\alpha = 0.30$						
$R^2 = 0.676$	$R^2 = 0.946$	$R^2 = 0.933$	$R^2 = 0.958$	$R^2 = 0.958$	$R^2 = 0.963$	
$Q^2 = 0.474$	$Q^2 = 0.598$	$Q^2 = 0.636$	$Q^2 = 0.649$	$Q^2 = 0.649$	$Q^2 = 0.668$	
SEE = 0.480	SEE = 0.205	SEE = 0.227	SEE = 0.182	SEE = 0.182	SEE = 0.171	
$F = 35$	$F = 114$	$F = 92$	$F = 128$	$F = 128$	$F = 146$	
$C = 3$	$C = 7$	$C = 7$	$C = 8$	$C = 8$	$C = 8$	
CoMFA and CoMSIA, ^c $\alpha = 0.30$						
					$R^2_{\text{test}} = 0.714$	
Model 2						
					$R^2 = 0.952$	
					$Q^2 = 0.691$	
					$R^2_{\text{test}} = 0.759$	
					SEE = 0.192	
					$F = 131$	

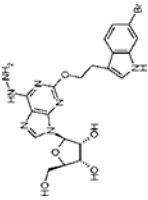
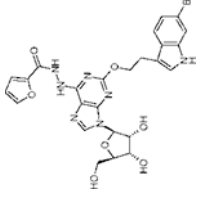
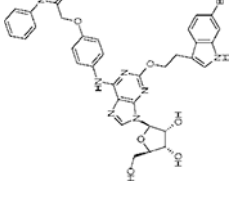
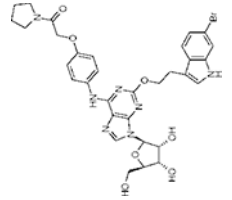
lattice space = 2 Å			
GH charge type	AM1 charge type	PM3 charge type	lattice space = 1 Å MINDO charge type
	CoMFA and CoMSIA, ^c $\alpha = 0.50$		$C = 7$
			Model 3
			$R^2 = 0.960$
			$Q^2 = 0.676$
			$R^2_{\text{test}} = 0.782$
			SEE = 0.175
			$F = 158$
			$C = 7$

^aGH, Gasteiger-Hückel; SEE, standard error of estimation; C, PLS components. The training set consisted of compounds 1–6, 12, 13, 15–17, 20–22, 24–26, 30–35, 37, 38, 40–48, 50–52, 54–56, 58, 60–62, 64–66, 68–70, 72–74, 76 (Supporting Information).

^bSteric, electrostatic, H-bond donor and acceptor CoMSIA regions were used; R, attenuation factor.

^cSteric, electrostatic, H-bond donor and acceptor, and hydrophobic CoMSIA regions were used; α , attenuation factor.

Table 2. Experimental and Predicted Potencies of the Novel Agonists in Activation of the Human A_{2B} AR and Experimental Binding Affinities Measured at Two Other ARs (EC₅₀ and K_i Values in nM)

Compound:	7	8	9	10
Structure:				
Functional data				
EC ₅₀ , A _{2B} ^a	174 ± 71	289 ± 48	143 ± 26	965 ± 424
RP (A _{2B}) ^a	-0.0944	-0.3148	-0.0092	-0.8384
RP (A _{2B}), Predicted ^b	-0.5000	-0.0828	0.8019	-0.4224
Binding data ^c				
K _i , A ₁	350 ± 65	29 ± 2% ^d	370 ± 150	420 ± 135
K _i , A _{2A}	2050 ± 600	40 ± 10% ^d	1150 ± 25	46 ± 7% ^d

^a Stimulation of adenylate cyclase measured in CHO cells stably expressing the human A_{2B} AR. RP: NECA **1** related potency. Compounds **7–10** appear to be full agonists compared to **1** at the A_{2B} AR (Supporting Information).

^b Using model 3 (Table 1).

^c Radioligand binding determined in CHO cell membranes (human A₁ AR) or in HEK293 cell membranes (human A_{2A}AR), as described in Experimental Section. K_i ± SEM values unless otherwise noted.

^d Percent displacement at 10 μM.